An iterative initialization scheme for mesoscale studies

By G. V. RAO and J. FISHMAN, *Department of Earth and Atmospheric Sciences, Saint Louis University, USA*

(Manuscript received April 24; revised version July 25, 1974)

ABSTRACT

An iterative technique to produce an initial set of consistent meteorological variables on a mesoscale basis is constructed. The development follows closely the earlier pioneering study of Miyakoda & Moyer (1968) who examined the feasibility of such a technique for synoptic scale initialization utilizing the linearized barotropic equations. The proposed scheme, on the other hand, employs the primitive equations of motion and emphasizes the three-dimensional structure. Another difference is the employment of a staggered grid which greatly facilitated the finite difference forms of the Laplacians and minimized some of the problems encountered in the earlier work. The present goal is to produce consistent sets of u, v, ω, ϕ, and θ-fields for subsequent mesoscale diagnosis. The structure of the various mesosystems, the horizontal and vertical subsynoptic circulations are studied. The immediate emphasis is not, however, on the examination of the initialized fields for possible use in prediction.

1. Introduction

A satisfactory understanding of the mesoscale motions can be gained by collecting good quality observations on that scale and by subjecting such data to sound dynamical treatments. For either diagnosis or prognosis on this scale, the wind-pressure relationship is likely to be better governed by the primitive equations than by some quasi-balanced approximations. Several dynamical meteorologists, e.g. Okland (1970) and Haltiner (1971) have stressed the importance of basing primitive equation predictions on properly initialized fields. The desirability of initialization will be more pressing if the area of intended forecast is small (e.g., small enough to resolve mesoconvective processes) and localized prognoses are demanded. Without proper initialization, the first few time integrations often yield very poor forecast fields as the data adjusts itself to the numerical model during this period.

Miyakoda & Moyer (1968) outlined an iterative initialization scheme for synoptic-scale motions. They used the linearized primitive barotropic equations of motion with a simple form of friction and controlled data. They enforced certain conditions on the time derivatives of the divergence field and allowed the initial fields to be adjusted through iterative time integration of the prediction equations. Euler's backward time differencing, which was shown by Matsuno (1966) to damp high frequency oscillations, was employed. Although this iterative scheme's deficiences had been cited previously (Nitta & Hovermale, 1969; Temperton, 1973) it was found that the utilization of a staggered grid minimized these weaknesses.

The purpose of this article is to discuss the development of a scheme based on a set of multilevel primitive equations to initialize mesoscale data. The most effective way of checking out an initialization technique is to subject the initialized fields through a time integration and observe the evolution of the meteorological fields. For reasons of economy and also because the present model is not intended to describe the complete dynamics of the mesoscale, a temporal integration is not attempted here. Instead the model structures of certain mesosystems like mesohighs, etc., are compared with those subjectively anlyzed. A favorable comparison was interpreted as a satisfactory evidence for initialization.

2. Computational procedures

The basic equations used in this research are:
(*a*) the momentum equations

$$\frac{\partial u}{\partial t} = -u\frac{\partial u}{\partial x} - v\frac{\partial u}{\partial y} - \omega\frac{\partial u}{\partial p} + fv - \frac{\partial \phi}{\partial x}$$

$$\frac{\partial v}{\partial t} = -u\frac{\partial v}{\partial x} - v\frac{\partial v}{\partial y} - \omega\frac{\partial v}{\partial p} - fu - \frac{\partial \phi}{\partial y}$$

(*b*) the equation of continuity

$$\frac{\partial u}{\partial x} + \frac{\partial v}{\partial y} + \frac{\partial \omega}{\partial p} = 0$$

(*c*) the hydrostatic equation, and

$$\frac{\partial \phi}{\partial p} = -\frac{RT}{p}$$

(*d*) the adiabatic equation

$$\frac{\partial \theta}{\partial t} = -u\frac{\partial \theta}{\partial x} - v\frac{\partial \theta}{\partial y} - \omega\frac{\partial \theta}{\partial p} \tag{1}$$

The above adiabatic and frictionless equations constitute the equation set (I).

The primary task is to iterate a modelled form of the above equations until an equilibrium state is reached between the fields of geopotential and momentum within certain prescribed tolerances. Since a diagnosis of the initial fields, as opposed to their prognosis is contemplated, presently a marching ahead in time is not needed. The procedure is as follows.

If the geopotential is the only primary input, eqs. (1) expressed in the finite difference form cannot be solved because the number of unknowns (e.g., u_{t_0}, v_{t_0}, etc.) exceeds the number of equations. Miyakoda & Moyer demanded the following restrictions on the divergence field

$$\chi_{t_0} = \chi_{t_0+2\Delta t} = \chi_{t_0+2\Delta t}$$

to form a closed set of equations.[1] In the above, χ is the velocity potential. The above requirement implies that the horizontal velocity components u and v are related to ψ the stream-function and χ in the following manner:

$$u = -\frac{\partial \psi}{\partial y} + \frac{\partial \chi}{\partial x};\ v = \frac{\partial \psi}{\partial x} + \frac{\partial \chi}{\partial y} \tag{2}$$

The equation for the vertical component of vorticity is utilized to solve for ψ:

$$\nabla^2\psi = \left(\frac{\partial v_1}{\partial x} - \frac{\partial u_1}{\partial y}\right) + \Delta t\left[\left(\frac{\partial u_0}{\partial x} + \frac{\partial v_0}{\partial y}\right)\eta_0 + \frac{\partial \omega_0}{\partial x}\frac{\partial v_0}{\partial p} - \frac{\partial \omega_0}{\partial y}\frac{\partial u_0}{\partial p} + u_0\frac{\partial \eta_0}{\partial x} + v_0\frac{\partial \eta_0}{\partial y} + \omega_0\frac{\partial \eta_0}{\partial p}\right] \tag{3}$$

where

$$\eta_0 \equiv \frac{\partial v_0}{\partial x} - \frac{\partial u_0}{\partial y} + f \text{ and}$$

the subscripts 0 and 1 are used to signify quantities at the initial time t_0 and one time step later, $t_0 + \Delta t$ respectively.

The above equation is obtained through cross-differentiation of eqs. 1 and writing

$$\frac{\partial}{\partial t}\nabla^2\psi = \frac{\nabla^2\psi_1 - \nabla^2\psi_0}{\Delta t} \quad \text{where } \nabla^2\psi = \frac{\partial v}{\partial x} - \frac{\partial u}{\partial y}$$

Eq. (3) also signifies taking a backward time step from $t_0 + \Delta t$ to t_0 to get an improved estimate of the rotational part of the wind (see also Haltiner, 1971, p. 258).

Eqs. (1) in their respective iterative form can be expressed as

$$u_1^* = u_0 + \Delta t\left(-u_0\frac{\partial u_0}{\partial \chi} - v_0\frac{\partial u_0}{\partial y} - \omega_0\frac{\partial u_0}{\partial p} + fv_0 - \frac{\partial \phi_0}{\partial x}\right) \tag{4}$$

$$\omega^*_{1(k-1)} = \omega^*_{1(k)} + \Delta p \bar{D}^*_{1(k,k-1)} \tag{5}$$

where

$$D = \frac{\partial u}{\partial x} + \frac{\partial v}{\partial y} \text{ and } \bar{D}_{(k,k-1)} = \frac{D_{(k)} + D_{(k-1)}}{2} \tag{6}$$

$$\theta_1^* = \theta_0 + \Delta t\left(-u_0\frac{\partial \theta_0}{\partial x} - v_0\frac{\partial \theta_0}{\partial y} - \omega_0\frac{\partial \theta}{\partial p}\right) \tag{7}$$

$$\text{and } \phi^*_{1(k-1)} = \phi^*_{1(k)} + \frac{R\Delta p}{P(k) + P(k-1)}\left(T^*_{1(k)} + T^*_{1(k-1)}\right) \tag{8}$$

Quantities denoted by a star (*) are temporary

[1] Support for an extension of the Miyakoda & Moyer constraint to the mesoscale comes from the various studies by Barnes (1974) who found the divergence pattern to retain its consistency prior to and during the outbreak of severe weather.

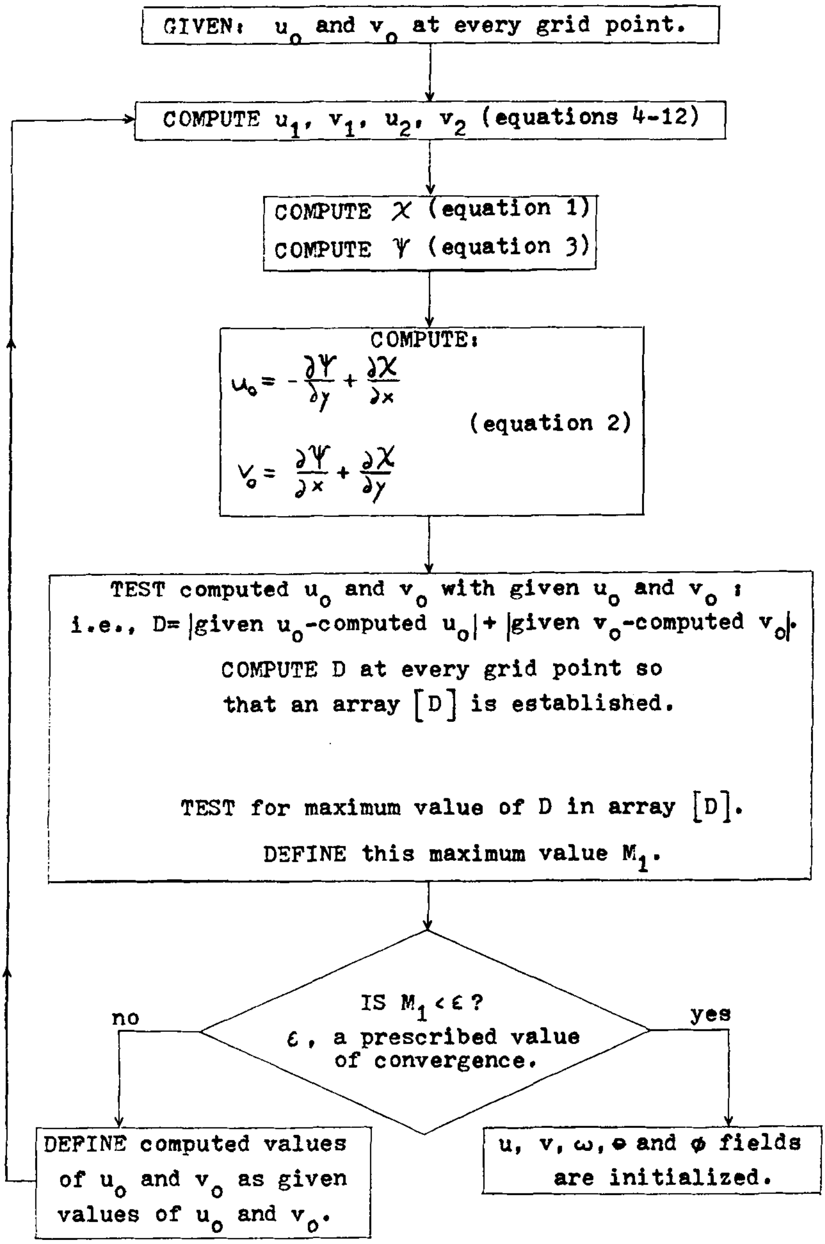

Fig. 1. Flow diagram for current initialization scheme.

computations necessary for Euler-backward time differencing; the subscript k refers to the kth isobaric level and $k = 1$ signifies the lowest pressure level. Following Miyakoda & Moyer (1968), u, v, ω, θ and ϕ are thus determined for the first time step:

$$u_1 = u_0 + \Delta t\left(-u_1^* \frac{\partial u_1^*}{\partial x} - v_1^* \frac{\partial u_1^*}{\partial y} - \omega_1^* \frac{\partial u_1^*}{\partial p} + f v_1^* - \frac{\partial \phi_1^*}{\partial x}\right) \tag{9}$$

$$\omega_{1(k-1)} = \omega_{1(k)} + \Delta p \bar{D}_{1(k,\,k-1)} \tag{10}$$

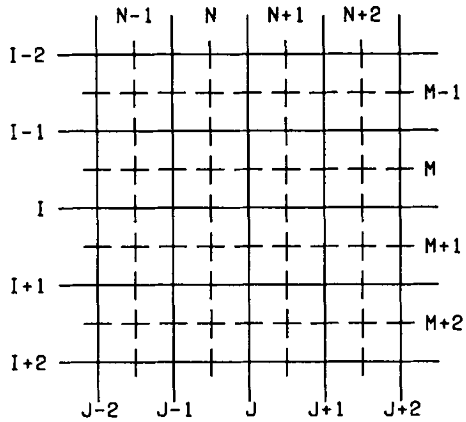

Fig. 2. A staggered grid on an isobaric surface. J increases eastward and I increases southward. The positioning of the various meteorological variables is described in the text.

$$\theta_1 = \theta_0 + \Delta t\left(-u_1^*\frac{\partial\theta_1^*}{\partial x} - v_1^*\frac{\partial\theta_1^*}{\partial y} - \omega_1^*\frac{\partial\theta_1^*}{\partial p}\right) \tag{11}$$

$$\text{and } \phi_{1_{(k-1)}} = \phi_{1_{(k)}} + \frac{R\Delta p}{P_{(k)} + P_{(k-1)}}(T_{1_{(k)}} + T_{1_{(k-1)}}) \tag{12}$$

It may be noted that the respective equations for v_1^* and v_1 are not written because of their similarity with u_1^* and u_1. u_2 and v_2 are likewise computed and with (1), a new χ-field is generated. Further, a new ψ-field is produced from u_1, v_1 and (3). Then (2) is solved for u_0 and v_0 on an isobaric lattice; these more recent u_0 and v_0 are compared with the corresponding values immediately prior to the iteration. If they vary within a prescribed tolerance limit between two successive iterations, the scheme is said to have converged. It is these converged wind components which are presented for diagnostic analysis and are numerically consistent in this model with the corresponding temperature and geopotential fields. Fig. 1 schematically displays the convergence criteria for the current initialization procedure.

According to Miyakoda & Moyer (1968), the Laplacians in (1) and (3) are written in a conventional lattice with a grid distance Δs as

$$\nabla^2 A_{(I,J)} = \left(\frac{1}{2\Delta s}\right)^2 [A_{(I+2,J)} + A_{(I-2,J)} + A_{(I,J+2)} + A_{(I,J-2)} - 4A_{(I,J)}] \tag{13}$$

for any quantity A. Unfortunately, (13) slows the convergence and sets up certain unwanted oscillations in the A-field near the boundaries contaminating perhaps the interior as the iteration proceeds. Furthermore, additional boundary values need be prescribed and the effective area of integration is reduced. Miyakoda & Moyer circumvented these problems by artificially smoothing the observed geopotential on the perimeter.

It has been found that these disadvantages which pertain to the slow convergence rates and the development of spurious oscillations can be minimized through the employment of a staggered grid shown in Fig. 2. The meteorological variables are arranged thus: Values for θ, ϕ and ψ will be positioned at the intersection of I and J,
χ and ω at M and N,
u at M and J,
v at I and N,

In this grid,

$$\nabla^2\chi_{(M,N)} = \frac{1}{(\Delta s)^2}[\chi_{(M+1,N)} + \chi_{(M-1,N)} + \chi_{(M,N+1)} + \chi_{(M,N-1)} - 4\chi_{(M,N)}]$$

since

$$\hat{u}_{(M,J)} = \frac{\chi_{(M,N)} - \chi_{(M,N-1)}}{\Delta s}$$

$$\text{and} \quad \hat{v}_{(I,N)} = \frac{\chi_{(M-1,N)} - \chi_{(M,N)}}{\Delta s}$$

where $\hat{u}$ and $\hat{v}$ represent the divergent part of the wind.

An analogous form for $\nabla^2\psi$ is similarly constituted.

Boundary values were formulated by a method similar to Hawkins & Rosenthal (1965, version 2) modified for a staggered grid. Fig. 3 shows an approximate layout of the National Severe Storms Laboratory mesoscale network (Barnes et al., 1971) as it existed in 1967. On this is superimposed the staggered grid with variables arranged in conformity with Fig. 2. An artificial outer boundary on which χ was set to zero was established. Then using the relationship that $\nabla^2\chi = \nabla\cdot\mathbf{V}$ was solved on the interior points. Denoting the direction along and perpendicular to the boundary by s and n, respectively, the ψ's on the inner boundary

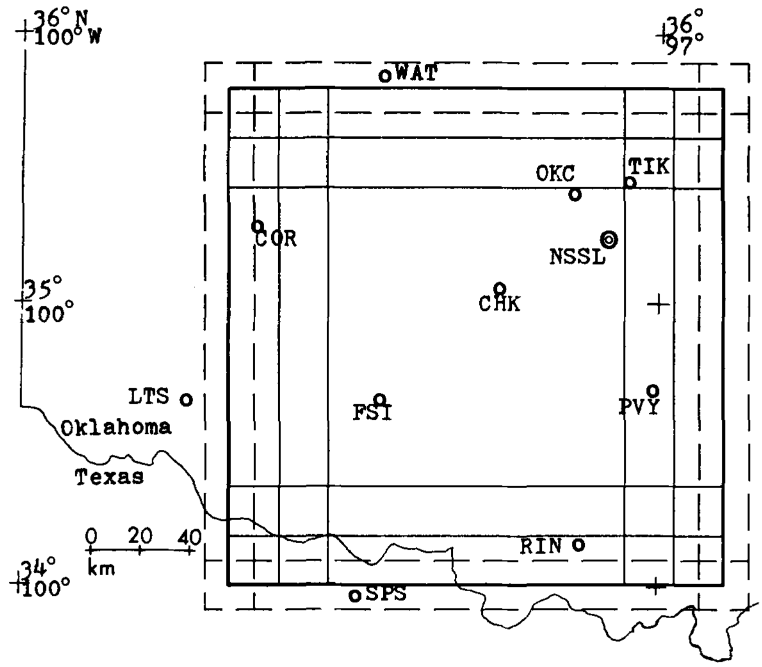

Fig. 3. National Severe Storms Laboratory mesonetwork in 1967 (Barnes et al., 1971) with the staggered grid superimposed. Heavier solid line outlines the area of integration for the numerical model. Outer dashed line is an artificial outer boundary described in the text. Dots show the position of the radiosonde release points.

are generated from the equation

$$\frac{\partial \psi}{\partial s} = V_n + \frac{\partial \chi}{\partial n}$$

from the observed V_n. The streamfunctions on the outer boundary were calculated using the relationship

$$\frac{\partial \psi}{\partial n} = V_s - \frac{\partial \chi}{\partial s}.$$

A simple arithmetic mean of the two adjacent points of each one of the four corners gives ψ's at the four corner points.

Mesoscale data (Fankhauser, 1969) were used to test the feasibility of the above model with $\Delta x = \Delta y = 20$ km and $\Delta p = 100$ mb. 1 000 mb constituted the bottom while 200 mb represented the top level because no mesoscale data were available at 100 mb and up.

Because the observed wind analyses were used to formulate the boundary values of ψ and χ a kinematic calculation of vertical velocities based on the boundary ψ and χ's produced unrealistically large values, particularly at upper levels. It was feared that such poor estimates would eventually contaminate the interior computations. Consequently an adjustment of the verticl velocities not only on the perimeter, but in the interior was made in a manner originally developed by O'Brien (1970) and described by Fankhauser (1969) and is as follows:

The improved vertical velocity ω' at any level k is written as

$$\omega'_{(k)} = \omega_{(k)} - (\omega_u - \omega_a)\frac{(L+1-k)(L+2-k)}{L(L+1)} \qquad (k = 1(1)L)$$

where L, the total numbers of levels is 9, ω_u and ω_a are the unadjusted (calculated using eq. 10) and adjusted vertical velocities at the top ($k=1$). The latter are obtained by multiplying by a constant ($\leqslant 1$) which sets the resulting mean equal to that of Fankhauser. Such an adjustment also facilitated a fairer

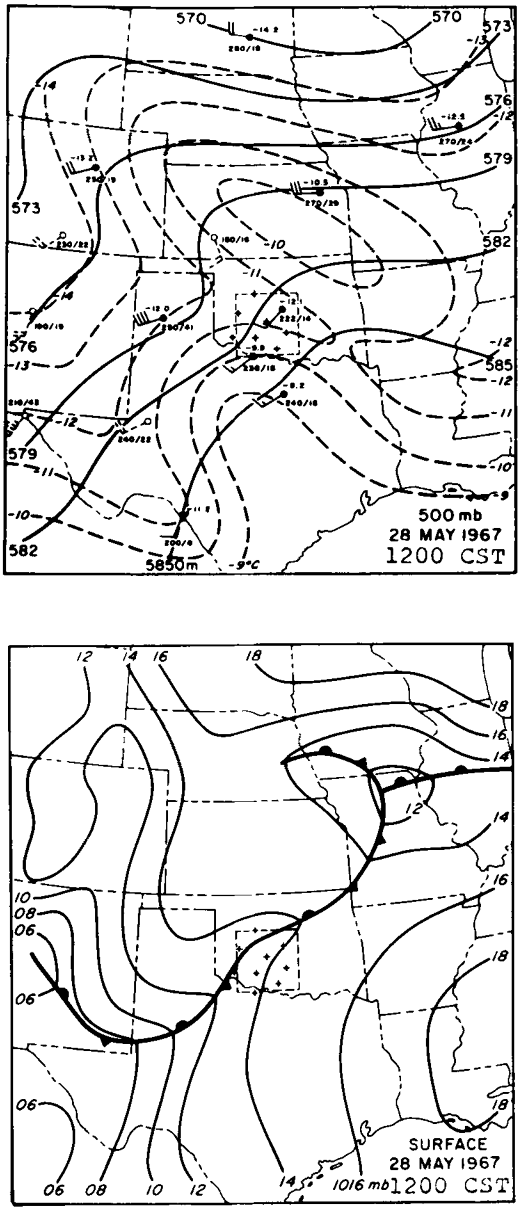

Fig. 4. Top: a 500-mb map showing the geopotential height contours (solid) and temperature (dashed). Winds are in knots, dashed barbs represent upper winds at nearest standard level. Bottom: a surface map showing the mesonetwork (boxed) and a quasi-stationary front (from Fankhauser, 1969).

comparison of the current ω's with those of Fankhauser.

Computation of ω at 1 000 mb was achieved by combining the frictionally and terrain-induced components of vertical velocity. Smoothed terrain contours with respect to the mean sea level (Schaefer, 1973) were employed.

The convergence of the wind field indicated by M_1 of Fig. 1, between two successive iterations at a point determines the equilibrium state of the model. When the present iterative technique was applied to a mesoscale situation (not described here) where no conspicuous discontinuities in the wind field were present, M_1 converged to less than 10 cm sec^{-1}. For the current situation, M_1 reached a value of 75 cm sec^{-1} and remained approximately the same for several iterations (5 or so) and then slowly increased. The initialized wind field is that which is obtained for a quasi-constant M_1.

Miyakoda & Moyer (1968) found that the initialized fields were fairly insensitive to the time step Δt used and that for the synoptic scale, Δt's as large as 1 440 sec converged. In the current 20-km model, a time step of 70 sec was the largest value which allowed convergence. For convenience, $\Delta t = 60$ sec was employed.

3. The data

The National Severe Storms Laboratory (NSSL) mesonetwork is situated in southwestern Oklahoma with its headquarters at Norman. Norman is skewed slightly (see Fig. 3) toward the climatological upwind (southwest) direction, with respect to the surface network to compensate for balloon displacement during flight (Barnes et al, 1971). An operational period extending from 15 April to 15 June was selected to cover Oklahoma's climatic peak in thunderstorm activity.

The case study of 28 May 1967 was chosen for this experiment because of the availability of the surface and radiosonde data and a detailed mesoanalysis of this situation from Fankhauser (1969). Fankhauser had originally selected this situation because on this day, the usual ingredients giving rise to thunderstorm formation, such as potential instability and vertical wind shear were only marginally present. Attention was purposely restricted by him to a situation of this type in an attempt to resolve the inherent limitations of the sounding system.

Close examination of the individual soundings, as well as the relative positions of soundings and radar echoes indicated that none of the released balloons entered thunderstorms. Thus, the measurements in the analyses can be regarded as representative of the external air mass environment.

Six hourly analyses of the wind, temperature, and moisture fields between 1 200 and 1 700 CST were available for the current study for every 50-mb from 950 through 20 mb. These analyses served as the input data for the initialization scheme.

The synoptic situation over the central United States is shown in Fig. 4. Of interest is the boxed area. A quasi-stationary front straddles across its northwestern part while a rather weak southwesterly flow exists aloft.

Echoes developed along the aforementioned front by 1 100 CST. Two hours later, their expanded versions were situated well within the mesonetwork. Thunderstorms continued in this area through the evening with the most severe storms occurring between 1 300 and 1 600 CST (Fankhauser, 1969). Thus, the situation of 1 400 was selected for initialization because of its representation of the mesoscale thunderstorm environment.

4. Results

Presence of upward vertical motion is a prerequisite for the occurrence of most weather phenomena. The vertical velocity is usually calculated by the kinematic, adiabatic or vorticity methods or by solving a vertical velocity (ω) equation. Presentation of the ω-field is of primary importance when objectively discussing the validity of a diagnostic analysis.

The 900-mb ω-vield (Fig. 5) reveals that the predominant area of upward motion parallels the qnasi-stationary front and regions of slight downward motion are closely aligned with the mesohighs depicted at the surface. According to Purdom (1973) a favored area for convective activity coincides with the intersection of a mesohigh and a quasi-stationary front. Supporting his observation, the center of strongest upward motion is developed in a corresponding area producing a definitive thunderstorm at 1 500 CST.

An examination of the 500-mb ω-field in the same figure discloses that the ascent associated with the aforementioned 1 500 CST thunderstorm area remains fairly constant in intensity in the vertical but suffers an eastward tilt. The downward motion in the north and south central parts of the diagram are associted with the two mesohighs. The descent related to the

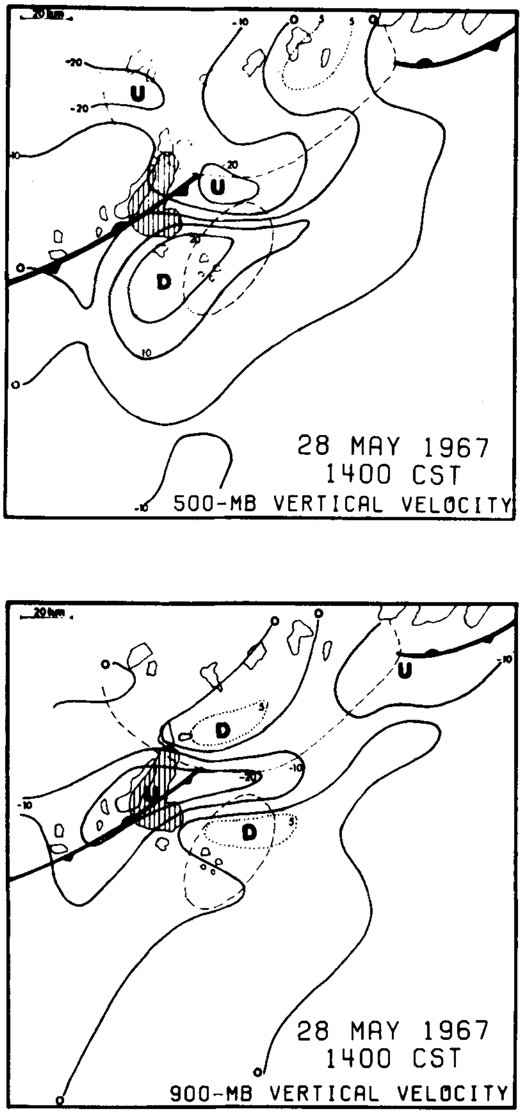

Fig. 5. ω-field with surface mesoanalysis. Units are microbars sec^{-1}. U and D signify centers of upward and downward motion, respectively. Irregular outlines depict radar echoes at the map time while hatched are the most intense radar echo an hour later. Thin dashed lines represent surface mesohighs.

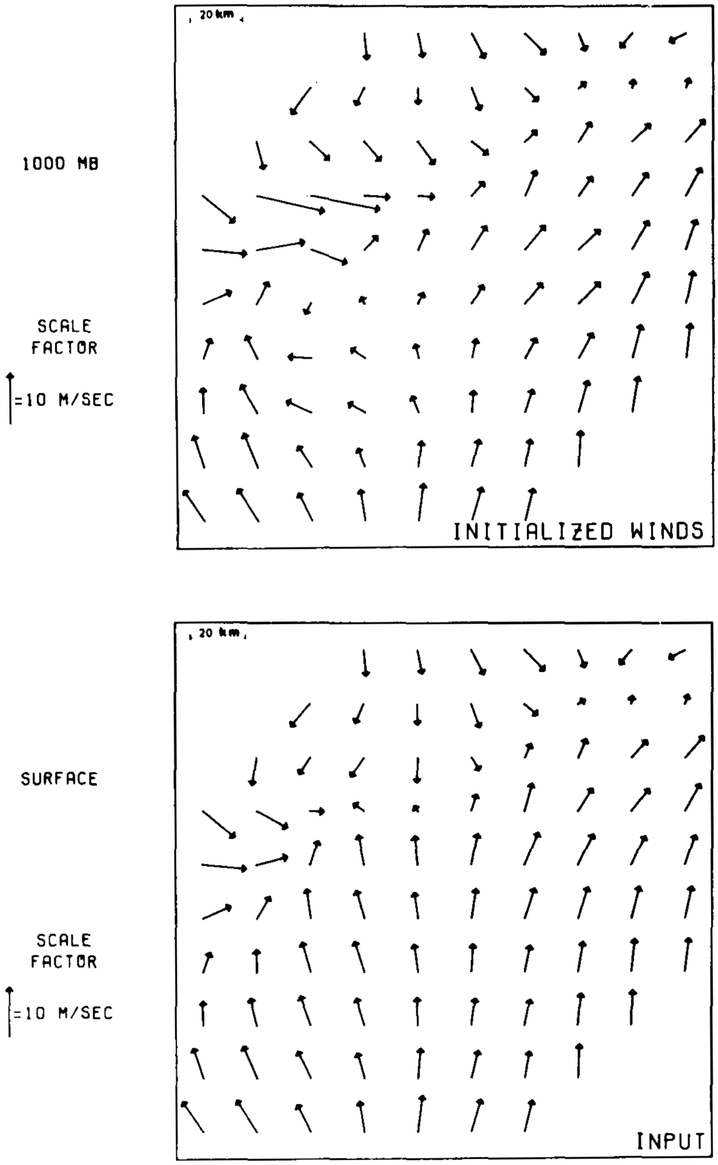

Fig. 6. The model derived 1 000-mb (initialized) and the subjectively analyzed surface winds. The latter served as the input to produce the 1000-mb wind field. Vectors originate at grid points.

northern mesohigh vanishes at 500 mb while that pertaining to the southern one has increased considerably both in area and intensity at this level. The weaker north-eastern ascent appears to the shallow. This region is so close to the periphery, however, that this calculation could be highly sensitive to boundary conditions.

To note the general agreement in the location of the ascent center, the present estimates are compared with those obtained earlier by Fankhauser (1969, Fig. 14). The latter's ω-analysis reveals a maximum upward motion at both 900 and 450 mb whereas it remains nearly constant through 500 mb in the current study. The descent associated with the mesohighs at 900 mb in Fig. 5 is not present in his analysis.

The construction of a 1 000-mb wind field

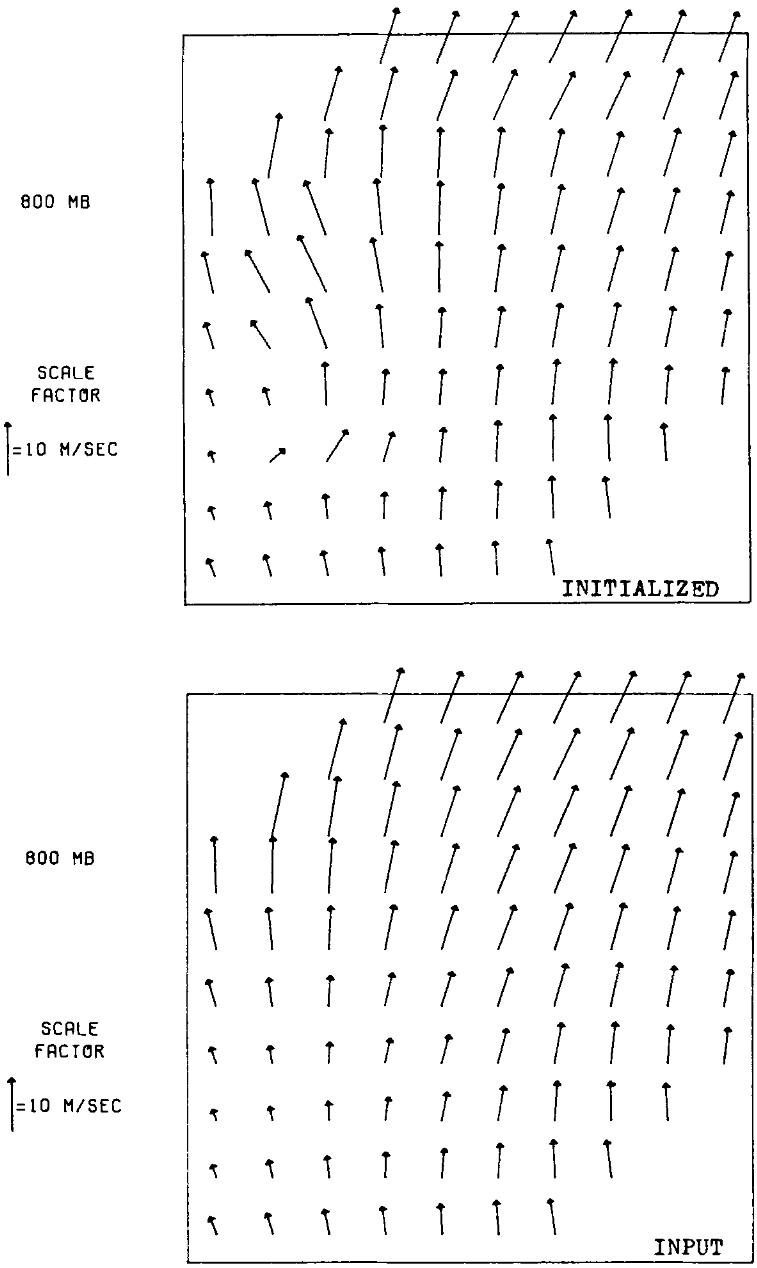

Fig. 7. The model derived (top) and the input (bottom) winds for 800-mb.

as demanded by the model is somewhat fictitious since the mesonetwork stations reported surface pressures ~ 970 mb. Because the model is frictionless, some deviation of the 1 000-mb winds from the surface winds may be expected. Fig. 6 shows a pronounced departure of the model winds from those observed in the west central part of the network. Demanding a certain consistency between the mass and momentum fields along with the frictionless

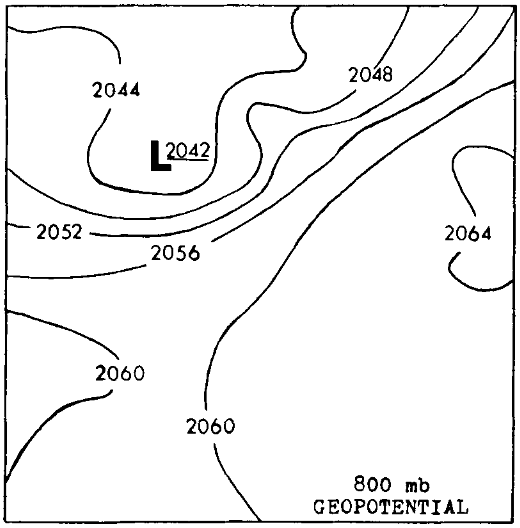

Fig. 8. The subjectively analyzed 800-mb geopotential field (m) for 1 400 CST 28 May 1967.

assumption perhaps accounts for the discrepancy. This area coincides with the region of most intense convective activity.

Fig. 7 shows the 800-mb wind field. The initialized winds, in general, are stronger and are more southerly. From Figs. 7 and 8 one concludes that the wind is blowing across the geopotentials, particularly in the west central part. Such a cross-contour flow and the lack of agreement between the vorticity (inferred from the flow pattern) and the pressure fields was also observed earlier by Tepper (1950), Fujita (1963), and Staff members (1963) and more recently confirmed by numerous investigators, e.g., Barnes (1973).

The deviation between the initialized and input winds became less with elevation, presumably because of the existence of less complicated pressure patterns and diminished role of friction.

5. Summary

The above discussion demonstrates the feasibility of extending the original Miyakoda & Moyer (1968) iterative scheme to a nine-level numerical model based on the primitive equations to investigate some mesoscale structures. The incorporation of a staggered grid into the model improved the computation, simplified the formulation of boundary conditions, and necessitated no smoothing on the perimeter.

The convergence qualities of this experiment are very encouraging although the complexity of the structure of the mesosystems limits the degree of convergence on this scale. Further refinements on the model, especially the inclusion of friction and other processes will hopefully yield an even better equilibrium state. Formulation of boundary conditions more consistent with the dynamics of the mesoscale situation is another area of improvement to be dealt with in future research.

Although O'Brien's (1970) special adjustment was incorporated into the model primarily to make a valid comparison with Fankhauser's (1969) results, it turned out that realistic ω's in the upper levels could not have been computed without it. In general, the analysies obtained in this study agree with those of Fankhauser.

Two noteworthy differences are the low-level descent associated with the mesohighs and the fairly uniform ascent through 500 mb. Fankhauser previously observed no low-level downward motion but dual ascent maxima at 900 and 450 mb in the same general region.

Acknowledgments

The authors wish to thank Professors Y. J. Lin and D. E. Martin for helpful discussions and also Mr J. C. Fankhauser of the National Center for Atmospheric Research (NCAR) for providing much of the data and valuable advice. Dr S. L. Barnes of the National Severe Storms Laboratory and Dr K. Miyakoda of the Geophysical Fluid Dynamics Laboratory offered useful suggestions on a preliminary version of this article. Appreciation is accorded to Mrs Fran Brummell for typing and Mr Wm. T. McDonald for photographing the illustrations.

The research is supported by the Atmospheric Sciences Section of the National Science Foundation under grant GA 26029 and by grant P4-3-022-35 from the National Severe Storms Laboratory. The National Center for Atmospheric Research sponsored by the NSF provided some of the computer time for this research.

REFERENCES

Barnes, S. L. 1974. Analysis of the thunderstorm structure and interaction with ambient atmosphere. *Colloquium on subsynoptic extratropical weather systems.* National Center for Atmospheric Research, Boulder, Colorado.

Barnes, S. L. 1973. Radar-observed merger of twin hook echoes. *Proceedings of the Eighth Conference on Severe Local Storms.* American Meteorological Society, Boston, pp. 155–160.

Barnes, S. L., Henderson, J. H. & Ketchum, R. H. 1971. Rawinsonde observation and processing techniques at the National Severe Storms Laboratory. *NOAA Technical Memorandum ERL NSSL-53*, Norman, Okla., 248 pp.

Fankhauser, J. C. 1969. Concvective processes resolved by a mesoscale rawinsonde network. *J. Appl. Met. 8*, 778–798.

Fujita, T. T. 1963. Analytical mesometeorology: A review. *Meteor. Monographs 5*, 77–125.

Haltiner, G. J. 1971. *Numerical weather prediction.* Wiley, New York, 317 pp.

Hawkins, H. F. & Rosenthal, S. L. 1965. On the computation of stream functions from the wind field. *Mon. Wea. Rev. 93*, 245–252.

Matsuno, T. 1966. Numerical integrations of the primitive equations by a simulated backward difference method. *J. Met. Soc. Japan 44*, 76–84.

Miyakoda, K. & Moyer, R. W. 1968. A method of initialization for dynamical weather forecasting. *Tellus 20*, 115–128.

Nitta, T. & Hovermale, J. B. 1969. A technique of objective analysis and initialization for the primitive forecast equations. *Mon. Wea. Rev. 97*, 652–658.

O'Brien, J. J. 1970. Alternative solutions to the classical vertical velocity problem. *J. Appl. Met. 9*, 197–203.

Okland, H. 1970. On the adjustment toward balance in primitive equation weather prediction models. *Mon. Wea. Rev. 98*, 271–279.

Purdom, J. F. W. 1973. Satellite imagery and the mesoscale convective forecast problem. *Proceedings of the Eighth Conference on Severe Local Storms.* American Meteorological Society, Boston, pp. 244–251.

Schaefer, J. T. 1973. On the computation of the surface divergence field. *J. Appl. Met. 12*, 546–547.

Staff members, National Severe Storms Project, 1963: Environmental and thunderstorm structures as shown by National Severe Storms Project observations in Spring 1960 and 1961. *Mon. Wea. Rev. 91*, 271–292.

Temperton, C. 1973. Some experiments in dynamic initialization for a simple primitive equation model. *Quart. J. Roy. Met. Soc. 99*, 303–319.

Tepper, M. 1950. A proposed mechanism of squall lines: the pressure jump line. *J. Meteor. 7*, 21–29.

ИТЕРАЦИОННАЯ СХЕМА ИНИЦИАЛИЗАЦИИ ДЛЯ МЕЗОМАСШТАБНЫХ ИССЛЕДОВАНИЙ

Строится итерационная техника для воспроизведения начального состояния согласованных метеорологических переменных на мезомасштабной основе. Построение тесно примыкает к более ранним пионерским исследованиям Миякоды и Мойера (1968), которые изучали возможности такой техники для инициализации процессов синоптического масштаба, используя линеаризированные баротропные уравнения. Предложенная схема с другой стороны использует примитивные уравнения движения и делает акцент на трехмерной структуре. Другое отличие состоит в использовании сетки с переменным шагом, что сильно облегчает конечноразностную аппроксимацию лапласианов и минимизирует некоторые проблемы, возникавшие в более ранней работе. Цель настоящей работы состоит в построении согласованных наборов полей u, v, ω, φ и θ для последующего мезомасштабного диагноза. Изучается структура различных мезосистем, а также горизонтальные и вертикальные субсиноптические циркуляции. Однако при изучении инициализации полей не делается акцента на возможном использовании техники в задачах прогноза.